We can't solve problems by using the same kind of thinking we used when we created them.

Albert Einstein

WORLD – UNIVERSE MODEL

MULTICOMPONENT DARK MATTER

COSMIC GAMMA-RAY BACKGROUND

Vladimir S. Netchitailo

Biolase Inc., 4 Cromwell, Irvine CA 92618, USA. v.netchitailo@sbcglobal.net

ABSTRACT

World – Universe Model is based on two fundamental parameters in various rational exponents: Fine-structure constant α, and dimensionless quantity Q. While α is constant, Q increases with time, and is in fact a measure of the size and the age of the World.

The Model makes predictions pertaining to masses of dark matter (DM) particles and explains the diffuse cosmic gamma-ray background radiation as the sum of contributions of multicomponent self-interacting dark matter annihilation.

The signatures of DM particles annihilation with predicted masses of 1.3 TeV, 9.6 GeV, 70 MeV, 340 keV, and 3.7 keV, which are calculated independently of astrophysical uncertainties, are found in spectra of the diffuse gamma-ray background and the emission of various macroobjects in the World.

The correlation between different emission lines in spectra of macroobjects is connected to their structure, which depends on the composition of the core and surrounding shells made up of DM particles. Thus the diversity of Very High Energy (VHE) gamma-ray sources in the World has a clear explanation.

1. INTRODUCTION

In 1937, Paul Dirac proposed a new basis for cosmology: the hypothesis of a time varying gravitational "constant" [1]. In 1974, Dirac added a mechanism of continuous creation of matter in the World [2]:

- *One might assume that nucleons are created uniformly throughout space, and thus mainly in intergalactic space. We may call this* ***additive creation****.*
- *One might assume that new matter is created where it already exists, in proportion to the amount existing there. Presumably the new matter consists of the same kind of atoms as those already existing. We may call this* ***multiplicative creation****.*

World – Universe Model (WUM) follows these ideas, albeit introducing a different mechanism of matter creation [3, 4]:

- Generation of particle – antiparticle pairs is occurring at the Front (the moving World – Universe boundary) due to high surface energy density of the Universe.
- Stable particles with lifetimes longer than the age of the World: protons, electrons, photons, neutrinos, and dark matter particles continue on into the World.
- The Front has a temperature invariant surface enthalpy $\sigma_0 = \frac{hc}{a^3}$ (h is Planck constant, c is the electrodynamic constant, a is the radius of the World's Nucleus at the Beginning: $a = 2\pi a_0$ and a_0 is the classical electron radius.).
- Amount of energy added to the World is proportional to the increase of the area of the Front. The total amount of the World energy is thus $E_W = 4\pi R^2 \sigma_0$, where $R = ct$ is the radius of the World at time t.

According to WUM, all stable particles, including all types of dark matter particles, are created at the Front. Dark matter particles include three Majorana fermions (neutralinos, WIMPs, and sterile neutrinos) and two spin-0 bosons (DIRACs and ELOPs), as detailed below.

2. DARK MATTER PARTICLES

Wikipedia states that *there are three prominent hypotheses on nonbaryonic DM, namely Hot Dark Matter (HDM), Warm Dark Matter (WDM), and Cold Dark Matter (CDM). The most widely discussed models for nonbaryonic DM are based on the CDM hypothesis, and corresponding particles are most commonly assumed to be Weakly Interacting Massive Particles (WIMPs)* [Wikipedia, Dark matter].

A neutralino with mass m_N *in* $100 \Leftrightarrow 10{,}000\ GeV/c^2$ *range is the leading DM candidate* [Wikipedia, Neutralino]. *Light Dark Matter Particles that are heavier than WDM and HDM but lighter than the traditional forms of CDM (neutralino) are DM candidates too. Their masses* m_{WIMP} *fall into* $1 \Leftrightarrow 10\ GeV/c^2$ *range* [Wikipedia, Light dark matter]. Subsequently, we will refer to light dark matter particles as WIMPs.

It is known that a sterile neutrino with mass m_{ν_s} *in* $1 \Leftrightarrow 10\ keV/c^2$ *range is a good WDM candidate* [Wikipedia, Warm dark matter]. *The best candidate for the identity of HDM is neutrino* [Wikipedia, Hot dark matter]. In our opinion, a tauonic neutrino is a good HDM candidate.

In addition to three fermions (neutralinos, WIMPs, sterile neutrinos) described above, the World – Universe Model offers another class of DM particles – spin-0 bosons, consisting of two fermions each. There are two types of DM bosons:

- DIRACs possessing mass of $m_0 = \frac{h}{ac} \cong 70\ MeV/c^2$ that are in fact magnetic dipoles
- ELOPs having mass of $\frac{2}{3}m_e \cong 340\ keV/c^2$ – preon dipoles (m_e is the electron mass).

Dissociated DIRACs can only exist at nuclear densities or at high temperatures. A DIRAC breaks into two Dirac's monopoles with mass $m_{mon} \gtrsim 35\ MeV/c^2$ and charge $\mu = \frac{e}{2\alpha}$ (e is the electron charge). In our opinion, these monopoles are the smallest building blocks of fractal structures of constituent quarks and hadrons [3, 4].

ELOPs break into two preons whose mass m_{pr} approximately equals to one third of an electron's mass: $m_{pr} \gtrsim 170\ keV/c^2$ and charge $e_{pr} = \frac{1}{3}e$. Preons are the smallest building blocks of fractal structures of quarks and leptons [3, 4].

We did not take into account the binding energies of DIRACs and ELOPs, and thus the values of the monopoles and preons masses are approximate. They have negligible electrostatic and electromagnetic charges because the separation between charges is very small. They do however possess non-negligible electrostatic and electromagnetic dipole momentum.

Multicomponent dark matter models consisting of both bosonic and fermionic components were analyzed in literature (for example, see [5-13] and references therein).

WUM postulates that masses of dark matter particles are proportional to m_0 multiplied by different exponents of α. Consequently, masses of various types of DM particles can be predicted:

Neutralinos:

$$m_N = \alpha^{-2} m_0 = 1.3149950\ TeV/c^2 \qquad 2.1$$

WIMPs:

$$m_{WIMP} = \alpha^{-1} m_0 = 9.5959823\ GeV/c^2 \qquad 2.2$$

DIRACs:

$$m_{DIRAC} = \alpha^{0} m_0 = 70.025267\ MeV/c^2 \qquad 2.3$$

ELOPs:

$$m_{ELOP} = \frac{2}{3}\alpha^{1} m_0 = 340.66606\ keV/c^2 \qquad 2.4$$

Sterile neutrinos:

$$m_{\nu_s} = \alpha^2 m_0 = 3.7289402 \ \ keV/c^2 \qquad 2.5$$

Above values fall into the ranges estimated in literature.

WUM holds that the relative energy densities of all types of DM particles are proportional to the relative proton energy density in the World's Medium:

$$\Omega_p = \frac{2\pi^2\alpha}{3} = 0.048014655 \qquad 2.6$$

In all, there are 5 different types of DM particles. Then the total energy density of DM is

$$\Omega_{DM} = 5\Omega_p = 0.24007327 \qquad 2.7$$

which is close to DM energy density discussed in literature: $\Omega_{DM} \cong 0.23$ [Wikipedia, Dark Matter].

Note that one of outstanding puzzles in particle physics and cosmology relates to so-called cosmic coincidence: the ratio of dark matter density in the World to baryonic matter density in the Medium of the World $\cong 5$ [13, 14].

Neutralinos, WIMPs, and sterile neutrinos are Majorana fermions, which partake in the annihilation interaction with strength equals to $\frac{1}{\alpha^2}$, $\frac{1}{\alpha}$, and α^2 respectively.

The main suggestion for experimentalists dealing with observations of Dark Matter is to concentrate their efforts on particles possessing masses shown above.

3. Macroobjects Built Up From Fermionic Dark Matter

Let's consider the possibility of all macroobject cores consisting of Dark Matter particles introduced in Section 2. In our view, all macroobjects of the World (including galaxy clusters, galaxies, globular clusters, extrasolar systems, and planets) possess the following properties:

- Macroobject cores are made up of DM particles;
- Macroobjects consist of all particles under consideration, in the same proportion as they exist in the World's Medium;
- Macroobjects contain other particles, including DM and baryonic matter, in shells surrounding the cores.

The first phase of stellar evolution in the history of the World may be Dark Stars, powered by Dark Matter heating rather than fusion. Neutralinos and WIMPs, which are their own antiparticles, can annihilate and provide an important heat source for the stars and planets in the World.

Table 1 summarizes the parameter values for Dark Stars made up of various fermions [3]:

Table 1

Fermion	Fermion relative mass m_f/m_0	Macroobject relative mass M_{max}/M_0	Macroobject relative radius R_{min}/L_g	Macroobject relative density ρ_{max}/ρ_0
Muonic neutrino	$Q^{-\frac{1}{4}}$	$Q^{\frac{1}{2}}$	$Q^{\frac{1}{2}}$	Q^{-1}
Tauonic neutrino	$6 \times Q^{-\frac{1}{4}}$	$6^{-2} \times Q^{\frac{1}{2}}$	$6^{-2} \times Q^{\frac{1}{2}}$	$6^4 \times Q^{-1}$
Sterile neutrino	α^2	α^{-4}	α^{-4}	α^8
Preon	$3^{-1}\alpha^1$	$3^2\alpha^{-2}$	$3^2\alpha^{-2}$	$3^{-4}\alpha^4$
Electron-proton (white dwarf)	α^1, β	β^{-2}	$(\alpha\beta)^{-1}$	$\alpha^3\beta$
Monopole	2^{-1}	2^2	2^2	2^{-4}
WIMP	α^{-1}	α^2	α^2	α^{-4}
Neutralino	α^{-2}	α^4	α^4	α^{-8}
Interacting WIMPs	α^{-1}	β^{-2}	β^{-2}	β^4
Interacting neutralinos	α^{-2}	β^{-2}	β^{-2}	β^4
Neutron (star)	$\approx \beta$	β^{-2}	β^{-2}	β^4

where

$$M_0 = \frac{4\pi m_0}{3} \times Q^{\frac{3}{2}} \tag{3.1}$$

$$L_g = a \times Q^{\frac{1}{2}} \tag{3.2}$$

$$\rho_0 = \frac{hc}{a^4} \tag{3.3}$$

The maximum density of neutron stars equals to the nuclear density

$$\rho_{max} = (\frac{m_p}{m_0})^4 \rho_0 = \beta^4 \rho_0 \tag{3.4}$$

which is the maximum possible density of any macroobject in the World (m_p is the proton mass).

A Dark Star made up of heavier particles – WIMPs and neutralinos – could in principle have a much higher density. In order for such a star to remain stable and not exceed the nuclear density, WIMPs and neutralinos must be Majorana fermions and partake in an annihilation interaction.

According to WUM, all macroobjects of the World (galaxies, stars, planets) possess cores made up of Dark Matter particles. The theory of fermion compact stars (FCS) made up of Dark Matter particles is well developed. Scaling solutions are derived for a free and an interacting Fermi gas [3].

Table 2 describes the parameters of FCS made up of different fermions:

Table 2

Fermion	**Fermion mass** $m_f, MeV/c^2$	**Macroobject mass** M_{max}, kg	**Macroobject radius** R_{min}, m	**Macroobject density** $\rho_{max}, kg/m^3$
Tauonic neutrino	4.50×10^{-8}	8.4×10^{50}	3.7×10^{24}	3.8×10^{-24}
Sterile neutrino	3.73×10^{-3}	1.2×10^{41}	5.4×10^{14}	1.8×10^{-4}
Preon	$\gtrsim0.17$	5.9×10^{37}	2.6×10^{11}	7.8×10^{2}
Monopole	$\gtrsim35$	1.4×10^{33}	6.2×10^{6}	1.4×10^{12}
Interacting WIMPs	9,596	1.9×10^{30}	8.6×10^{3}	7.2×10^{17}
Interacting neutralinos	$1{,}315\times10^{3}$	1.9×10^{30}	8.6×10^{3}	7.2×10^{17}
Electron/proton (white dwarf)	0.511/938.3	1.9×10^{30}	1.6×10^{7}	1.2×10^{8}
Neutron (star)	939.6	1.9×10^{30}	8.6×10^{3}	7.2×10^{17}

The calculated parameters of FCS show that

- White Dwarf Shells (WDS) around the nuclei made of strongly interacting WIMPs or neutralinos compose cores of stars in extrasolar systems;
- Shells of Dissociated DIRACs to Monopoles around the nuclei made of strongly interacting WIMPs or neutralinos form cores of globular clusters;
- Shells of Dissociated ELOPs to Preons around the nuclei made of strongly interacting WIMPs or neutralinos constitute cores of galaxies;
- Shells of Sterile neutrinos around the nuclei made of strongly interacting WIMPs or neutralinos make up cores of galaxy clusters;
- Shells of Tauonic neutrinos around the nuclei made of strongly interacting WIMPs or neutralinos reside in the cores of galaxy superclusters.

Although there are no free Dirac's monopoles and preons in the World, they can arise in the cores of FCS as the result of DIRACs and ELOPs gravitational collapse with density increasing up to the nuclear density ($\sim 10^{17}\ \frac{kg}{m^3}$) and/or at high temperatures, with subsequent dissociation of dipoles to monopoles and preons.

The existence of supermassive objects in galactic centers is now commonly accepted. It is commonly believed that the central mass is a supermassive black hole. There exists, however, evidence to the contrary.

In late 2013, ICRAR astronomer Dr. Natasha Hurley-Walker spotted a previously unknown radio galaxy NGC1534 that is quite close to Earth at 248 million light years, but is much fainter than it should be if the central black hole was accelerating the electrons in the jets:

The discovery is also intriguing because at some point in its history the central black hole switched off but the radio jets have persisted. This is a very rare occurrence—this is only the fifth of this type to be discovered, and by far the faintest. We can only see it at low frequencies, which tells us that the electrons in the jets are not getting new energy from the black hole, so it must have been switched off for some time [65].

It's also possible there was never a black hole there at all.

Alternative models for the supermassive dark objects in galactic centers, formed by self-gravitating non-baryonic matter composed of fermions and bosons, are widely discussed in literature.

According to WUM, the heaviest macroobjects include a high-density preon plasma shell around their cores:

- Macroobjects with a cold preon shell emit strong radio waves. Such objects are good candidates for the compact astronomical radio sources at centers of galaxies like Sagittarius A* in the Milky Way Galaxy [Wikipedia, Sagittarius A*].
- Red Giants are macroobjects with hot preon shells.
- Blazars are members of a larger group of active galaxies that host active galactic nuclei (AGN) [Wikipedia, Blazar]. They are macroobjects with hot preon and sterile neutrinos shells.
- Quasars are the most energetic and distant members of AGN. They are macroobjects with very hot preon and sterile neutrinos shells.
- Seyfert galaxies are one of the two largest groups of AGN, along with quasars. They have quasar-like nuclei, but unlike quasars, their host galaxies are clearly detectable. Seyfert galaxies account for about 10% of all galaxies [Wikipedia, Seyfert galaxy].

Note that the temperature of the preon and sterile neutrinos shells depends on the composition of the macroobject core. Macroobjects whose cores are made up of WIMPs and preons remain cold. Macroobjects with cores made up of WIMPs and WDS produce hot preon and sterile neutrino shells. Macroobjects whose cores consist of neutralinos and WDS have very hot preon and sterile neutrino shells.
The mass of an AGN is about 7-11 orders of magnitude larger than the mass of the Sun. The radius of an AGN is about 4-7 orders of magnitude larger than the radius of WDS (see Table 2). The area of the closed spherical surface around the AGN is 8-14 orders of magnitude greater than the surface area of WDS. Luminosity of the AGN is then 8-14 orders of magnitude higher than the luminosity of the Sun.

This take on an AGN explains the fact that *the most luminous quasars radiate at a rate that can exceed the output of average galaxies, equivalent to two trillion (2×10^{12}) suns* [Wikipedia, Quasar].

To summarize, macroobjects of the World have cores made up of DM particles. The cores are surrounded by shells made up of DM and baryonic matter. Every macroobject consists of all particles under consideration that are present in the same proportion as they exist in the World's Medium. No compact stars are made up solely of DM fermionic particles, for instance.

4. X Rays and Gamma Rays

All "elementary" particles of the World are fermions and they possess masses. Bosons such as photons, X-quants, and gamma-quants are composite particles and consist of two fermions.

Gamma rays are usually distinguished from X rays by their origin: *X rays are emitted by electrons outside the nucleus, while gamma rays are emitted by the nucleus* [Wikipedia, Gamma ray]. A better way to distinguish the two, in our opinion, is the type of fermions composing the core of X-quants and gamma-quants.

Super-soft X rays [Wikipedia, Super-soft X-ray source] possess energies in the 0.09 $\Leftrightarrow$ 2.5 keV range, whereas soft gamma rays have energies in the 10 $\Leftrightarrow$ 5000 keV range. We assume that X-quants are composed of two interacting neutrinos. It possesses rest mass of $m_X \sim m_0 \times Q^{-\frac{1}{4}}$, which is decreasing with time: $m_X \propto t^{-\frac{1}{4}}$ [3, 4]. New Physics with the dineutrinos in the Rare Decay $B \to K\nu\bar{\nu}$ is actively discussed in literature in recent years (for example, see [15, 16]).

Soft gamma-quants are composed of two sterile neutrinos ($3.7\ keV$ each). Hard and super-hard gamma-quants may be composed of two preons ($\gtrsim$ 0.17 MeV each), which are ELOPs in our Model, two Dirac's monopoles ($\gtrsim 35\ MeV$ each) which are, in fact, DIRACs.

We propose that Super-soft gamma rays ($< 10\ keV$) can arise as the result of sterile neutrino annihilation in the low energy case. Two or three super-soft gamma-quants with the energy $< 3.7\ keV$ are created. Similarly,

- ELOP annihilation produces soft gamma rays with energies $< 340\ keV$
- DIRAC annihilation produces hard gamma rays with energies $< 70\ MeV$
- WIMP annihilation produces very-hard gamma rays with energies $< 9.6\ GeV$
- Neutralino annihilation produces super-hard gamma rays with energies $< 1.3\ TeV$.

Diffuse cosmic gamma-ray background is the sum of the contributions of the multicomponent self-interacting dark matter annihilation.

5. Dark Matter Signatures in Gamma-Ray Spectra

Large number of papers has been published in the field of X-ray and gamma-ray astronomy. The X-ray and gamma-ray background from $\lesssim 0.1\ keV$ to $\gtrsim$ 10 TeV has been studied using high spectral and spatial resolution data from different spectrometers. Numerous papers were dedicated to Dark Matter searches with astroparticle data (for example, see reviews [17-26] and references therein).

Dark Matter annihilation is proportional to the square of the DM density and is especially efficient in places of highest concentration of dark matter, such as compact stars built up from fermionic dark matter particles (see Section 3).

Recall that no macroobjects are made up of just a single type of DM particles, since other DM particles as well as baryonic matter are present in the shells. It follows that macroobjects cannot irradiate gamma rays in a single spectral range. On the contrary, they irradiate gamma-quants in different spectral ranges with ratios of fluxes depending on structure of a given macroobject.

The models of DM annihilation and decay for various types of macroobjects (galaxy clusters, blazars, quasars, Seyfert galaxies) are well-developed. Physicists working in the field X-ray and gamma-ray astronomy attempt to determine masses of DM particles that would fit the experimental results with the developed models.

WUM predicts existence of DM particles with 1.3 TeV, 9.6 GeV, 70 MeV, 340 keV, and 3.7 keV masses. We will look for signs of annihilation of these particles in the observed gamma-ray spectra. We connect gamma-ray spectra with the structure of macroobjects (its core and shells composition).

5.1. 1.3 TeV Neutralino

J. Holder has this to say about TeV Gamma-ray Astronomy:

Approximately 1% of all galaxies host an active nucleus; a central compact region with much higher than normal luminosity. Around 10% of these Active Galactic Nuclei (AGN) exhibit relativistic jets, powered by accretion onto a supermassive black hole. Blazars, which host a jet oriented at an acute angle to the line of sight, are of particular interest for gamma-ray astronomy, as the emission from these objects is dominated by relativistic beaming effects, which dramatically boost the observed photon energies and luminosity.

The mechanisms which drive the high energy emission from blazars remain poorly understood, and a full discussion is beyond the scope of this review. Briefly; in leptonic scenarios, a population of electrons is accelerated to TeV energies, typically through Fermi acceleration by shocks in the AGN jet. These electrons then cool by radiating X-ray synchrotron photons. TeV emission results from inverse Compton interactions of the electrons with either their self-generated synchrotron photons, or an external photon field. The strong correlation between X-ray and TeV emission which is often observed provides evidence for a common origin such as this, although counter examples do exist [27].

In our opinion, this correlation between X-ray (keV) and TeV emission can be easily explained by the annihilation of the sterile neutrinos (3.7 keV) in the shell around the core of AGN made of neutralinos (1.3 TeV). Moreover, the TeV blazar emission should be classified as extremely-hard X rays and not gamma rays, since by definition, *X rays are emitted by electrons outside the nucleus, while gamma rays are emitted by the nucleus.*

The gamma-ray emission with energy less than 1.3 TeV can be produced by annihilation or decay of stable DM particles with lifetimes $\sim 10^{27}\ s$ or larger [28] – much longer than the age of the World $\sim 10^{18}\ s$.

In our opinion, gamma-ray emission with energy exceeding 1.3 TeV is the result of interactions of highest energy particles observed in cosmic rays (mostly protons) with interstellar medium.

The authors of [28, 29] calculated *the upper limits on the velocity-weighted annihilation cross-section for direct annihilation into two photons, as a function of* m_χ, *from the Segue 1 observations with MAGIC. In almost the entire considered mass range, the upper limits are within* 1σ *from the null hypothesis; the largest deviation is observed at* $m_\chi \sim 1.3\ TeV$ *where the signal is slightly larger than* 2σ (Figure 1):

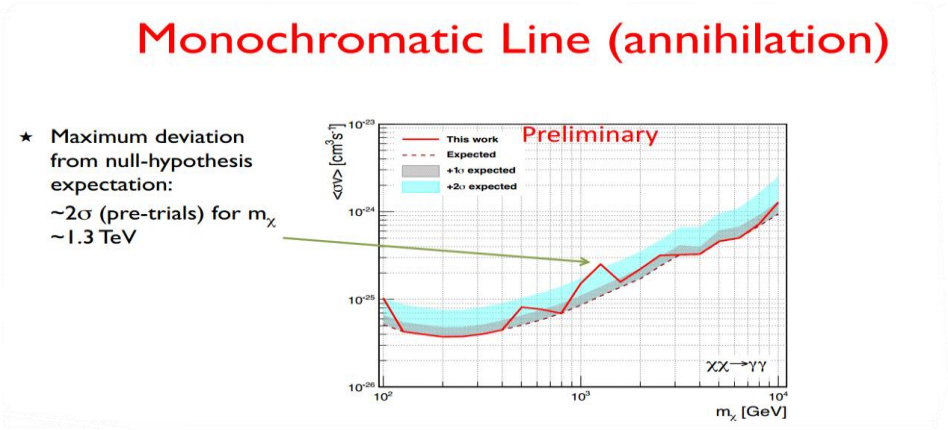

Figure 1. Upper limits on $\langle \sigma_{ann} v \rangle$ for direct annihilation into two photons, as a function of m_χ, from the Segue 1 observations with MAGIC (solid line) and as expected for the case of no signal (dashed line), as well as for a signal of 1σ or 2σ significance (gray and light blue shaded areas, respectively). Figure adapted from [29].

Figures 2 and 3 show monochromatic line of DM annihilation $m_{DM} \cong 1\ TeV$ from Galactic Halo observations with H.E.S.S. [28-30].

H. B. Jin, *et al.* performed a detailed global analysis on the interpretation of the latest data of PAMELA, Fermi-LAT, and AMS-02 in terms of dark matter annihilation and decay in various propagation models. They showed that for 2μ (muon) channel, the Fermi-LAT data alone favour $m_\chi \approx 1.3\ TeV$ [31]. This value of DM particle mass equals to the neutralino mass in our Model.

The total $e^+ + e^-$ flux was measured by FERMI-LAT, PAMELA, HESS, and other collaborations. *CALorimetric Electron Telescope (CALET) on International station is an astrophysics mission that searches for signatures of dark matter and provides the highest energy direct measurements of the cosmic ray electron spectrum in order to observe discrete sources of high energy particle acceleration in our local region of the Galaxy. Observation targets: Signatures in electron/gamma energy spectra in the 10 GeV – 10 TeV range* [40].

The distributions of the total $e^+ + e^-$ flux measured by FERMI-LAT, PAMELA, HESS, and other collaborations are shown in Figures 4 and 5.

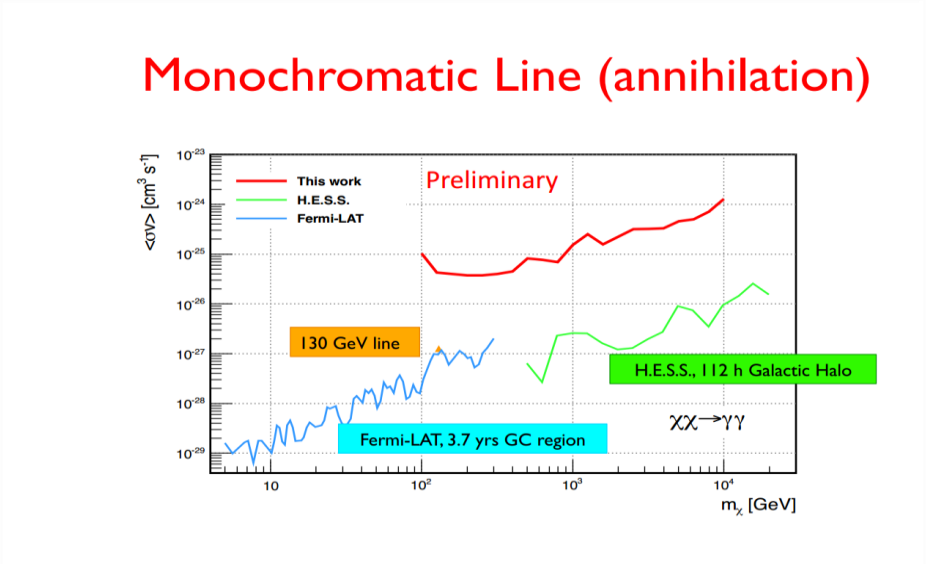

Figure 2. Upper limits on $\langle \sigma_{ann} v \rangle$ for direct annihilation into two photons, as a function of m_χ, from the Segue 1 observations with MAGIC and from Galactic Halo observations with H.E.S.S. Figure adapted from [29].

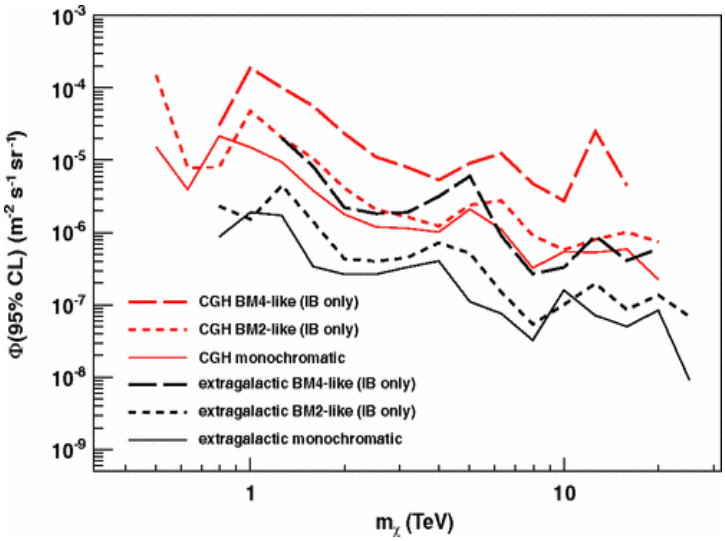

Figure 3. Flux upper limits on spectral features arising from the emission of a hard photon in the DM annihilation process. The monochromatic line limits, assuming $m_\chi = E_\gamma$, are shown for comparison. Figure adapted from [30].

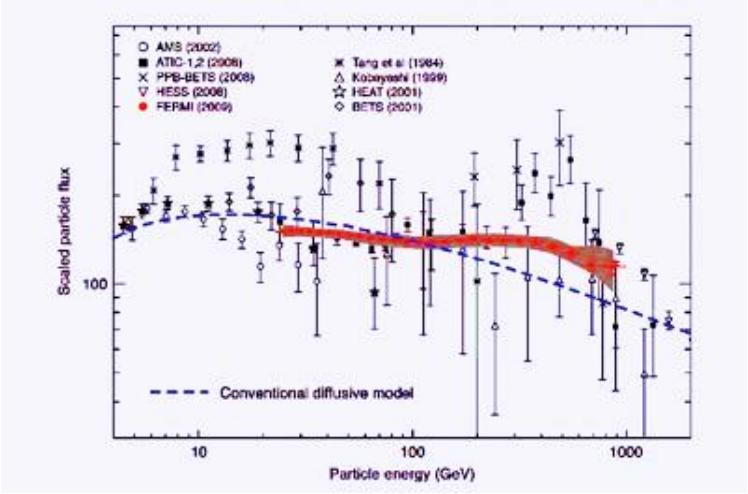

Figure 4. The Fermi LAT cosmic ray (CR) electron spectrum (red filled circles). Systematic errors are shown by the gray band. Other high-energy measurements and conventional diffusive model are shown. Figure adapted from [32].

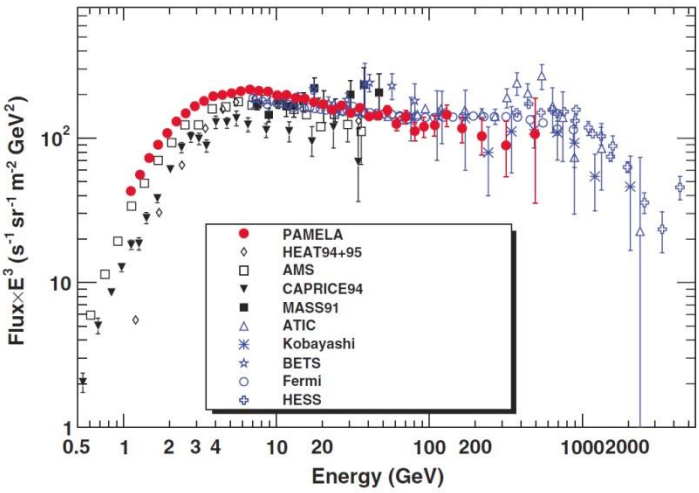

Figure 5. The electron energy spectrum obtained in this work (PAMELA) compared with modern measurements: CAPRICE94, HEAT, AMS, MASS91, Kobayashi, BETS, ATIC, HESS, Fermi. Note that the data points, indicated with blue symbols, and the highest data point from HEAT are for the electron and positron sum. The figure adapted from [33].

A. A. Abdo, *et al.* have this to say about Cosmic Ray $e^+ + e^-$ spectrum [32]: *The obtained spectra can be nicely fit by adding an additional component of primary electrons and positrons, with injection spectra* $J(E) \propto E^{-\gamma} exp\{-E/E_{cut}\}$ *with the spectral index* γ *of about 3 and* E_{cut} *being the cutoff energy of the source spectra. Such an additional component also provides a natural explanation of the steepening of the spectra above 1 TeV indicated by the obtained data. Pulsars are the most natural candidates for such sources.*

N. Kawanaka, *et al.* have this to say about cosmic ray spectrum: *we adopt the background model of exponentially cutoff power-law with an index of - 3.0 and a cutoff at 1.5 TeV, which is similar to that shown in Aharonian, et al. [39] and reproduces the data in* $\sim 10\ GeV - 1\ TeV$ *well* [38].

Diffuse gamma-ray results anticipated for CALET in five years of investigations compared to the previous data and to model predictions are depicted in Figure 6. The anticipated results are in a very good agreement with the predicted mass of neutralino.

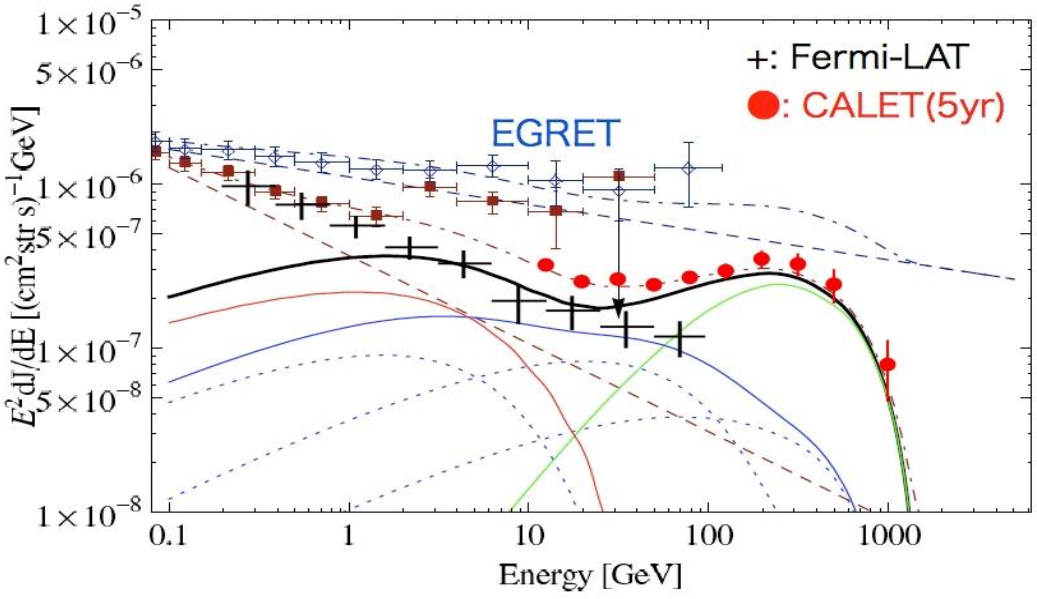

Figure 6. The total $e^+ + e^-$ flux measured by FERMI-LAT and CALET from a single pulsar surrounded by supernova remnant. Diffuse gamma ray results anticipated for CALET. Figure adapted from [40].

The mass of the annihilating DM serves as the cutoff scale of the $e^{\pm}$ spectrum. The lepton spectra must have a cutoff energy at the DM particle mass m_χ. The obtained data require DM mass to be around 1 to 1.5 TeV [32-40] which is in good agreement with the predicted mass of a neutralino (1.3 TeV).

R.C.G. Chaves, *et al.* have this to say about Extending the H.E.S.S. Galactic Plane Survey:

Approximately 100 VHE γ *-ray sources have now* (2009) *been discovered* [42-46]. *Over two-thirds of these sources are located in our Galaxy. VHE* γ *-rays carry information about the most extreme environments in the local Universe, and although a significant fraction of the Galactic VHE* γ *-ray sources do not appear to have obvious counterparts at other wavelengths, the majority of them are associated with the violent, late phases of stellar evolution, e.g. supernova remnants (SNRs), pulsar wind nebulae (PWNe) of high spin-down luminosity pulsars, and massive Wolf-Rayet (WR) stars in stellar clusters* [41].

O. Tibolla, *et al.* have this to say about New Unidentified H.E.S.S. Galactic Sources:

Some of the unidentified H.E.S.S. sources have several positional counterparts and hence several different possible scenarios for the origin of the VHE gamma-ray emission; their identification remains unclear. Others have so far no counterparts at any other wavelength. Particularly, the lack of an X-ray counterpart puts serious constraints on emission models [42].

As we mentioned above, pulsars are the most natural candidates for such VHE gamma-ray sources.

Wikipedia defines pulsar as a *highly magnetized, rotating neutron star that emits a beam of electromagnetic radiation. Neutron stars are very dense, and have short, regular rotational periods* [Wikipedia, Pulsar].

According to WUM, Fermionic Compact Stars made up of strongly interacting neutralinos and WIMPs have maximum mass and minimum size which are exactly equal to parameters of neutron stars (see Tables 1 and 2). It follows that pulsars might be in fact rotating Neutralino stars and WIMP stars with different shells around them.

The cores of such pulsars can also be built up from the mixture of neutralinos (1.3 TeV) and WIMPs (9.6 GeV) surrounded by shells composed of the other DM particles: DIRACs (70 MeV), ELOPs (340 keV), and sterile neutrinos (3.7 keV). Annihilation of those DM particles can give rise to any combination of gamma-ray lines. Thus the diversity of VHE gamma-ray sources in the World has a clear explanation in frames of the World – Universe Model.

5.2. 9.6 GeV WIMP

In his review "Empirical Case for 10 GeV Dark Matter" Dan Hooper summarized and discussed the body of evidence which has accumulated in favor of dark matter in the form of approximately 10 GeV particles, including *the spectrum and angular distribution of gamma rays from the Galactic Center, the synchrotron emission from the Milky Way's radio filaments, the diffuse synchrotron emission from the Inner Galaxy (the "WMAP Haze") and low-energy signals from the direct detection experiments DAMA/LIBRA, CoGeNT and CRESST-II.* Dan Hooper finds that *gamma-ray signal observed from the Galactic Center is consistent with 7-12 GeV dark matter particles annihilating mostly to leptons* [47].

WUM predicts the mass of a WIMP $m_{WIMP} = 9.6\ GeV$ independently of astrophysical uncertainties. Let's examine the experimentally measured masses of WIMPs and see how closely the fit our prediction.

Dan Hooper and Lisa Goodenough estimated Dark Matter Annihilation in the Galactic Center and found that it fits into 7-10 GeV range [42].

In their "EGRET Observations of the Extragalactic Gamma Ray Emission", P. Sreekumar, *et al.* provide a graph of the all-sky observations in high-energy gamma rays from 30 MeV to 100 GeV:

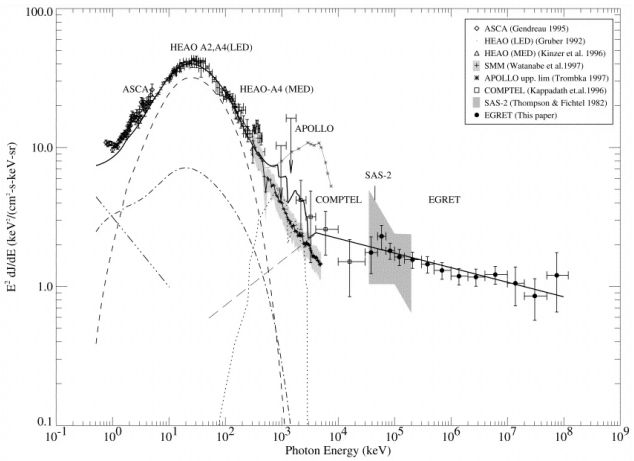

Figure 7. Multiwavelength spectrum of the extragalactic gamma rays; spectrum from X rays to high-energy gamma rays. The estimated contribution from Seyfert 1 (dot-dashed), and Seyfert 2 (dashed) are from the model of Zdziarski (1996); steep-spectrum quasar contribution (dot-dot-dashed) is taken from the paper of Chen et al. (1996); Type Ia supernovae (dot) is from the paper of Leising and Clayton (1993). The blazar contribution below 4 MeV (thin long dashed) is derived assuming the average blazar spectrum breaks around 4 MeV (McNaron-Brown, *et al.* 1995) to a power law with an index of ∼−1.7. The thick solid line indicates the sum of all the components. Figure adapted from [49].

EGRET data on diffuse gamma-ray background show visible peaks around 70 MeV and 10 GeV. 10 GeV peak is consistent with annihilation of WIMPs. 70 MeV peak corresponds to annihilation of DIRACs (Section 5.3).

Based on EGRET observations, P. Sreekumar, *et al.* attribute the high-energy gamma ray emissions to blazars. *Most of the measured spectra of individual blazars only extend to several GeV and none extend above 10 GeV, simply because the intensity is too weak to have a significant number of photons to measure* [49].

WUM proposes that cores of blazars are composed of annihilating WIMPs (9.6 GeV), explaining why no observed radiation extends above 10 GeV.

The results of gamma-ray emission between 100 MeV to 10 GeV detected from 18 globular clusters in our Galaxy are also in a good correlation with the predicted mass of WIMPs. The gamma-ray spectra are generally described by a power law with a cut-off at a few GeV (1.4 – 7.1 GeV) [50, 51].

The DAMA/LIBRA, CoGeNT, CRESST-II, CDMS-II collaborations conduct direct detections of DM particles by nuclear recoils due to the elastic scattering of DM particles. The closest result to the predicted mass of WIMPs was obtained by CDMS-II collaboration which has reported 3 events in Si detector that are consistent with being nuclear recoils due to scattering of Galactic dark matter particles. An 8.6 GeV DM particle is deemed most probable [52].

Based on its core assumptions, WUM analytically predicts WIMPs to possess the mass of 9.6 GeV. A large number of experimental results seem to converge around 10 GeV, providing additional support to WUM.

5.3. 70 MeV DIRAC

DIRAC is a spin-0 boson with 70 MeV mass. In our opinion, the DIRAC may indeed be the so-called U boson, target of intense search by the scientific community.

Observations of the cosmic electron and/or positron flux by ATIC, PAMELA, HESS, Fermi, and recently the AMS02 Collaboration have revealed an unexpected excess at momenta above 10 GeV, in particular in the positron fraction $e^+/(e^- + e^+)$. *These observations cannot easily be reconciled in a consistent way with known astrophysical sources and alternative theoretical explanations have therefore been put forward. In particular, scenarios in which the excess radiation stems from the annihilation of weakly interacting dark matter particles might offer an enticing solution to this puzzle.*

To accommodate Dark Matter (DM) in elementary particle theory and to allow it to interact with visible matter, it has been proposed to supplement the Standard Model (SM) with an additional sector characterized by another U(1)' gauge symmetry [54-57]. The corresponding vector gauge boson – called U boson, A', γ', or simply dark photon – would thereby mediate the annihilation of DM particles into charged lepton pairs. The mass of the U boson is thought to remain well below $1\ GeV/c^2$ *[58].*

In recent years, a number of such searches have been conducted in various experiments done in the few-GeV beam energy regime, looking either at e^+e^- *pair distributions produced in electron scattering [59, 60] or in the electromagnetic decays of the neutral pion [61, 62] and the* ϕ *meson [63, 64]. In a similar fashion the WASA-at-COSY experiment [62] has covered the mass range* $M_U = 0.02 - 0.1\ GeV/c^2$ *by investigating decays of* π^0 *produced in proton-induced reactions at 0.55 GeV beam energy* [53].

Note that the mass of DIRAC proposed by WUM $m_{DIRAC} = 0.07 GeV/c^2$ falls into the mass range of U boson: $M_U = 0.02 - 0.1\ GeV/c^2$.

C. Boehm, P. Fayet, and J. Silk propose a way to reconcile the low and high energy signatures in gamma-ray spectra:

It has recently (2003) *been pointed out that the 511 keV emission line detected by Integral/SPI from the bulge of our galaxy could be explained by annihilations of light Dark Matter particles into* e^+e^-. *If such a signature is confirmed, then one might expect a conflict with the interpretation of very high energy gamma rays if they also turn out to be due to Dark Matter annihilations.*

They point out *that it is possible to reconcile the low and high energy signatures, even if both of them turn out to be due to Dark Matter annihilations. One would be a heavy fermion for example, like the lightest neutralino (> 100 GeV [67]), and the other one a possibly light spin-0 particle (~ 100 MeV [67]). Both of them would be neutral and also stable as a result of two discrete symmetries (say R and M-parities)* [66].

According to WUM, the two coannihilating DM particles are

- Neutralino (1.3 TeV) – a heavy fermion, and
- DIRAC (70 MeV) – a light spin-0 boson.

In Section 5.1 we discussed the observations of gamma rays in the very high-energy (> 100 GeV) domain [28-42] which are consistent with self-annihilating neutralino. In Section 5.2 we showed multiwavelength spectrum of the extragalactic gamma rays (Figure 7) and mentioned the 70 MeV peak.

S. D. Hunter, *et al*. discuss a "pion bump" centered at 67.5 MeV:

Below about 100 MeV, gamma rays produced via electron bremsstrahlung are the dominant component of the observed spectrum, whereas, above about 100 MeV, the gamma-rays from π^0 *decay, which form the broad "pion bump" centered at 67.5 MeV, are the dominant component of the spectrum. The "pion bump ", clearly visible in this spectrum, is the only spectral feature in the diffuse gamma ray emission in the EGRET energy range* [68].

70 MeV peak in EGRET data was discussed by Golubkov and Khlopov [69]. They explained this peak by the decay of π^0-mesons, produced in nuclear reactions.

B. Wolfe, *et al.* said that gamma rays at 70 MeV are notably detectable by GLAST and EGRET [70].

Another example of 70 MeV peak in the emission spectrum from an old supernova remnant (SNR) is shown in Figure 8. R. Yamazaki, *et al.* attribute the peak to π^0-decay:

When the SNR age is around 10^5 *yrs., proton acceleration is efficient enough to emit TeV γ-rays both at the shock of the SNR and that in the giant molecular cloud (GMC). The maximum energy of primarily accelerated electrons is so small that TeV γ-rays and X-rays are dominated by Hadronic processes,* π^0*-decay and synchrotron radiation from secondary electrons, respectively.* [71, 72]

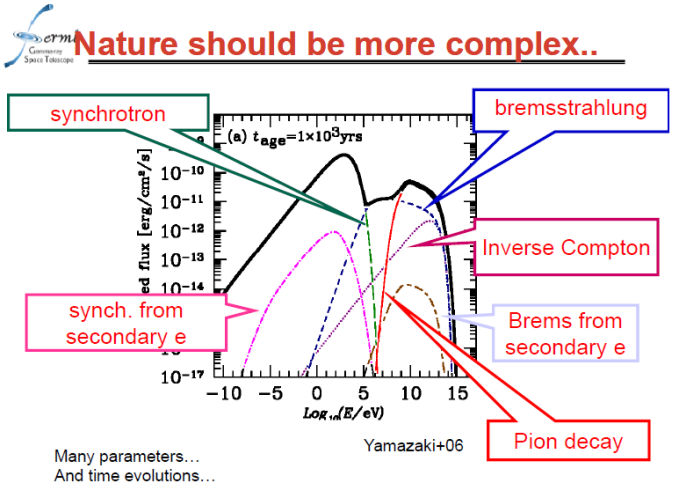

Figure 8. Spectrum of a single supernova remnant (SNR) with an age 1×10^3 years that stores energy, 10^{50} ergs, of high-energy protons. Figure adapted from [72].

Note that whenever the 70 MeV peak appears in gamma-ray spectra, it is always attributed to pion decay. We claim that π^0 decay produces a 67.5 MeV peak, while DIRAC annihilation is responsible for 70 MeV peak. Observation of the two distinct peaks is complicated by the broadness of the observed "pion bump".

We suggest utilization of exponentially cutoff power-law for analysis of experimental data for gamma-ray energies < 70 MeV. A better fit of experimental data will be evidence of DIRAC annihilation.

5.4. 340 KEV ELOP

An ELOP is a spin-0 boson with 340 keV mass. Existence of DM particles of similar masses has been discussed by Y. Rasera, *et al.*:

The cosmic gamma-ray background (CGB) between 10 keV and 10 GeV has been measured by several gamma-ray satellites (HEAO, SMM, COMPTEL and EGRET). Below 100 keV, it is believed that the main contribution comes from Seyfert galaxies. Above 10 MeV, a simple model for blazars reproduces both the amplitude and the slope of the data. In the intermediate energy range, however, another type of sources is needed, since blazar spectra show a clear break near 10 MeV and the cosmological gamma-ray background from Seyfert galaxies falls off above about 100 keV.

The diffuse gamma-ray background depends on three main quantities. The first is the annihilation cross-section: we are going to explore two extreme cases: S-wave and P-wave. The second ingredient is the dark matter mass density profile: we are going to test peaked distributions (Moore, c=15) and shallow ones (NFW, c=15). The last unknown quantity is the dark matter particle mass m_χ.

Both the NFW S-wave case and the Moore P-wave reproduce the total flux of the bulge 511 keV emission with reasonable Dark Matter particle mass of the order of $m_\chi \cong 100\ MeV$ *and* $m_\chi \cong 1\ MeV$ *respectively. On the opposite, the NFW P-wave case would require masses* ($m_\chi < 0.42\ MeV$) *so small that they are unable to produce 511 keV photons* [73].

The extragalactic background spectrum between 1 keV and 10 GeV is presented in Figure 9.

Figure 9 shows a visible "bump" around 4 keV (Section 5.5) and in the 100 – 400 keV range. The theoretical NFW P-wave case with mass $m_\chi < 0.42$ MeV discussed above [73] is in good agreement with the experimental 100-400 keV "bump" [74] and with annihilating ELOPs with mass 340 keV proposed in our Model [3, 4].

In our view, there are two coannihilating DM particles at play that explain these bumps:

- WIMP (9.6 GeV) – a heavy fermion, and
- ELOP (340 keV) – a light spin-0 boson.

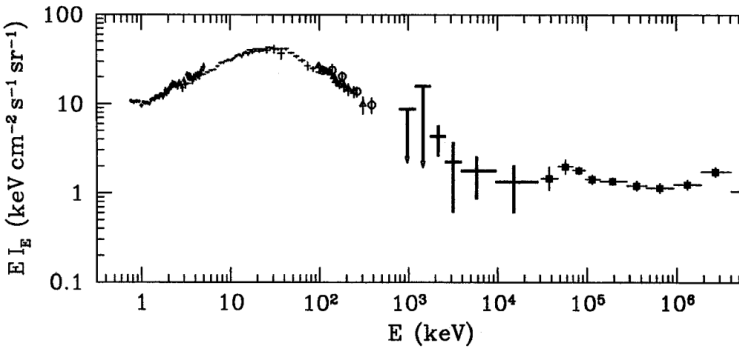

Figure 2. The high-energy extragalactic background spectrum from up-to-date measurements. The crosses marked b 5 keV show the *ASCA* data as given by Gendreau (1995). The *ASCA* spectrum includes a Galactic contribution, significa spectral feature at ~2 keV is of instrumental origin. Crosses in the 3–100 keV range are from *HEAO-1* A2 and A4 (Gruber 1992; see also Marshall et al. 1980; Rothschild et al. 1983). The data marked by open triangles and open circl A4 MED (Kinzer et al. 1996), and Nagoya balloon (Fukada et al. 1975) measurements, respectively. Note that both the A4 MED data suggest that the normalization of the *HEAO-1* A2/A4 LED spectrum is somewhat underestimated. Th 0.8–30 MeV range are from COMPTEL (Kappadath et al. 1995), and the filled squares denote the data from EGRET preparation).

Figure 9. Extragalactic background spectrum inspired by Figure 2 of A. A. Zdziarski [74].

D. E. Gruber, *et al.* describes a wide gamma-ray diapason as a sum of three power laws:

Above 60 keV selected data sets included the HEAO 1 A-4 (LED and MED), balloon, COMPTEL, and EGRET data. The fit required the sum of three power laws, the flattest of which largely characterizes the EGRET observations (it ignores a likely "ripple" at 70 MeV), and the next steeper, with index 1.58, may be said to represent the spectrum between 70 keV and 1 MeV. The steepest component, with index 5.5, is almost certainly only a numerical necessity for matching to the lower energy spectrum and its derivative, and represents nothing physical [75].

According to our Model, the fit of the total diffuse spectrum in the range between 3 keV and 10 GeV should be performed based on three exponentially cutoff power-laws with injection spectral $J(E) \propto E^{-\gamma} exp\{-E/E_{cut}\}$ with the spectral index γ and E_{cut} being the cutoff energy of the source spectra. For values of E_{cut}, we should use

- 9.6 GeV (annihilating WIMPs) in the 9.6 GeV – 70 MeV range;
- 70 MeV (annihilating DIRACs) in the 70 MeV – 340 keV range;
- 340 keV (annihilating ELOPs) in the 340 keV – 3.7 keV range.

The fit in the range between 9.6 GeV and 1.3 TeV should be done with $E_{cut} = 1.3\ TeV$, which equals to the mass of a neutralino.

5.5. 3.7 keV Sterile Neutrino

The Wikipedia overview of a sterile neutrino suggests the possibility of it being a Majorana fermion:

Unlike for the left-handed neutrino, a Majorana mass term can be added for a sterile neutrino without violating local symmetries (weak isospin and weak hypercharge) since it has no weak charge. However, this would still violate total lepton number.

It is possible to include both Dirac and Majorana terms: this is done in the seesaw mechanism. In addition to satisfying the Majorana equation, if the neutrino were also its own antiparticle, then it would be the first Majorana fermion (Wikipedia [Sterile neutrino]).

There are a lot of observations of the cosmic-ray radiation around 3.7 keV. In our opinion, gamma rays of this energy are radiated by annihilation of sterile neutrinos.

But even if this emission could be the result of decay of sterile neutrinos with twice the mass (7.4 keV), the cosmic radiation in 3.7 keV range is gamma-ray and not X-ray radiation.

The very first signature of the emission around 3.7 keV was found in 1967 by P. Gorenstein, R. Giacconi, and H. Gursky. In their "The Spectra of Several X-ray Sources in Cygnus and Scorpio" paper they analyzed the counting rate in the 2 – 5 keV range and found that *the sources GX-10.7, +9.1, +13.5, and +16.7 are qualitatively different from Sco X-1, Cyg X-1 or Cyg X-2 in that the highest number of net counts is recorded in the bin centered at 3.75 keV* [76].

An important result was obtained by S. Safi-Harb and H. Ogelman in 1997. In the "ROSAT and ASCA Observations of W50 Associated with the Peculiar Source SS 433" paper they reported that *the observations of the X-ray lobes of the large Galactic source W50 [are] associated with the two-sided jets source SS 433.*

They noted *that a continuum model (power law or thermal bremsstrahlung) plus a Gaussian improves the fit to region w2 slightly. However, a broken power-law model gives the best fit. The power-law indices are 1.9 and 3.6, with the break occurring at 3.7 keV. This result is also close to our findings for the spectral fitting of region e2 in the eastern lobe, except that the spectrum from the western lobe is softer* [77].

T. Itoh analyzed the broad-band (3.0–50 keV) spectra of NGC 4388 in his PhD Thesis "Suzaku Studies of Time Variable X-ray Spectra of Edge-On Active Galactic Nuclei" (2007). He wrote:
The ionized iron absorption line indicates the presence of an ionized reprocessing material in the line of sight, as well as the cold matter. At this point, there still remained line like residuals around 3.7 keV and 4.0 keV. We included two more Gaussians at these energies, to find that they are significant at similar levels as above [78].

A. M. Bykov, *et al.* confirm the 3.7 keV peak in their "Isolated X-ray – infrared sources in the region of interaction of the supernova remnant IC 443 with a molecular cloud":

The nature of the extended hard X-ray source XMMU J061804.3+222732 and its surroundings is investigated using XMM-Newton, Chandra, and Spitzer observations. The X-ray emission consists of a number of bright clumps embedded in an extended structured non-thermal X-ray nebula larger than 30" in size. Some clumps show evidence for line emission at ~ 1.9 keV and ~ 3.7 keV at the 99% confidence level. A feature at 3.7 keV was found in the X-ray spectrum of Src 3 at the 99% confidence level [79].

R. Fukuoka, *et al*. observed the peak as well:

In the 18'x18' field of view, we found four distinct X-ray sources: a bright star and a diffuse source associated with the star clusters in the soft band (0.5-2.0 keV), a small clump in a higher energy band (4-6 keV), and a peculiar clump in the 6.4 keV line band.

We found two line-like residuals at ~ 3.7 keV and ~ 3.0 keV. We therefore added two narrow Gaussians for these lines, and then obtained a nice fit. The first *line was surely detected with ~ 3σ significance* [80].

In 2012, A. Moretti, *et al*. measured the diffuse gamma-ray emission *at the deepest level and with the best accuracy available today* [81]. An emission like around 3.7 keV is clearly visible in Figure 10:

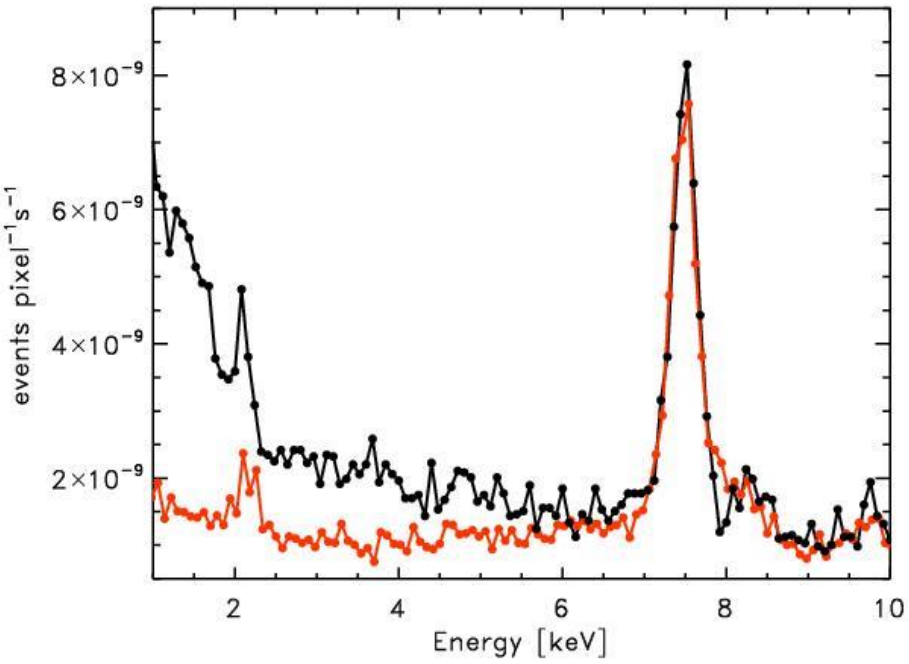

Figure 10. The energy channel (PI) distribution of the XPT unresolved emission (black) compared with the instrument background (red). In this plot PI channels have been transformed in energy using a single value and not the RMF matrix. The Figure adapted from [81].

6. Conclusion

- Emission line of 3.7 keV can be found in the spectrum of the diffuse gamma-ray background radiation and in spectra of different macroobjects of the World. WUM attributes this radiation to annihilation of sterile neutrinos in shells around cores of different macroobjects (Blazars, Quasars, Seyfert galaxies, etc.).
- The broken power-law with the break occurring at 3.7 keV bears witness to the change of the source of gamma radiation. In our opinion, ELOPs, which contribute to gamma-ray spectrum in 340 keV – 3.7 keV range, are replaced with sterile neutrinos in < 3.7 keV range.
- Emission lines of 1.3 TeV, 9.6 GeV, 70 MeV, 340 keV, and 3.7 keV, can be found in spectra of the diffuse gamma-ray background radiation and various macroobjects of the World in different combinations depending on their structure.
- The diffuse cosmic gamma-ray background radiation in the < 1.3 TeV range is the sum of the contributions of multicomponent self-interacting dark matter annihilation.
- The total cosmic-ray radiation consists of gamma-ray background radiation plus X-ray radiation from the different highly ionized chemical elements in the hot areas of the World and is due to various electron processes such as synchrotron radiation, electron bremsstrahlung, and inverse Compton scattering.

Acknowledgements

I am grateful to Felix Lev, my life-long friend, for our frequent discussions of history and philosophy of Physics. Special thanks to my son Ilya Netchitailo who questioned every aspect of the paper and helped shape it to its present form.

References

1. P. A. M. Dirac, Nature, **139**, 323 (1937).

2. P. A. M. Dirac, Proc. R. Soc. Lond. **A**., **338**, 439 (1974).

3. V. S. Netchitailo (2013), viXra: 1303.0077 v7.

4. V. S. Netchitailo (2014), viXra: 1401.0187 v2.

5. S. Arrenberg, H. Baer, V. Barger, L. Baudis, D. Bauer, J. Buckley, *et al.* (2013) http://www-public.slac.stanford.edu/snowmass2013/docs/CosmicFrontier/Complementarity-27.pdf

6. J. Heeck, H. Zhang (2013), arXiv: 1211.0538 v2.

7. M. Aoki, *et al.* (2012), arXiv: 1207.3318 v2.

8. A. Kusenko, M. Loewenstein, T. Yanagida, Phys. Rev. D **87**, 043508 (2013).

9. D. Feldman, Z. Liu, P. Nath, G. Peim (2010), arXiv: 1004.0649 v2.

10. J. L. Feng (2010), arXiv: 1003.0904 v2.

11. K. M. Zurek (2009), arXiv: 0811.4429 v3.

12. C. Boehm, P. Fayet, J. Silk (2003), arXiv: 0311143 v1.

13. W. Z. Feng, A. Mazumdar, P. Nath (2013), arXiv: 1302.0012 v2.

14. W. Z. Feng, P. Nath, G. Peim (2012), arXiv: 1204.5752 v2.

15. W. Altmannshofer, *et al.* (2009), arXiv: 0902.0160 v2.

16. P. Del Amo Sanchez, *et al.* (2011), arXiv: 1009.1529 v2.

17. L. E. Strigari (2012), arXiv: 1211.7090 v1.

18. K. Bechtol (2011) http://astro.fnal.gov/events/Seminars/Slides/Bechtol%20120611.pdf

19. J. H. Buckley, *et al.* (2008), arXiv: 0810.0444 v1.

20. T. Jeltema, 2011http://www2011.mpe.mpg.de/erosita/erosita2011/program/PDF/jeltema.pdf

21. F. A. Aharonian (2004) http://www.worldscientific.com/worldscibooks/10.1142/4657

22. T. Totani (2009) http://www-conf.kek.jp/past/HEAP09/ppt/1day/Totani_HEAP09.pdf

23. R. P. Johnson, R. Mukherjee, New J. Phys. **11**, 055008 (2009).

24. F. Giovanneli, L. Sabau-Graziati, Mem. S. A. It. **83**, 17 (2012).

25. R. Essig, *et al.* (2013), arXiv: 1309.4091 v3.

26. T. A. Porter, R. P. Johnson, P. W. Graham (2011), arXiv: 1104.2836 v1.

27. J. Holder (2012), arXiv: 1204.1267 v1.

28. J. Aleksic, *et al.* (2013), arXiv: 1312.1535 v3.

29. A. Moralejo (2013) http://projects.ift.uam-csic.es/multidark/images/moralejoalcala.pdf

30. A. Abramowski, *et al.* (2013), arXiv: 1301.1173 v1.

31. H. B. Jin, Y. L. Wu, Yu. F. Zhou (2013), arXiv: 0905.0025 v1.

32. A. A Abdo, *et al.* (2009), arXiv: 0905.0025 v1.

33. O. Adriani, *et al.* (2011), arXiv: 1103.2880 v1.

34. X. G. He (2009), arXiv: 0908.2908 v2.

35. I. Cholis, L. Goodenough (2010), arXiv: 1006.2089 v2.

36. A. Morselli, Progress in Particle and Nuclear Physics **66**, 208 (2011).

37. K. N. Abazajian, J. P. Harding (2011), arXiv: 1110.6151 v3.

38. N. Kawanaka, *et al.* (2010), arXiv: 1009.1142 v3.

39. F. A. Aharonian, *et al*., Phys. Rev. Lett. **101**, 261104 (2008).

40. D. Granger http://calet.phys.lsu.edu/Science/DGR.php

41. R. C. G. Chaves, *et al.* (2009), arXiv: 0907.0768 v1.

42. O. Tibolla, *et al.* (2009), arXiv: 0907.0574 v1.

43. S. Hoppe, *et al.* (2009), arXiv: 0906.5574 v2'

44. P. H. T. Tam, *et al.* (2009), arXiv: 0911.4332 v2.

45. O. Tibolla, *et al.* (2009), arXiv: 0912.3811 v1.

46. P. H. T. Tam, *et al.* (2010), arXiv: 1001.2950 v1.

47. D. Hooper (2012), arXiv: 1201.1303 v1.

48. D. Hooper, L. Goodenough (2010), arXiv: 1010.2752 v3.

49. P. Sreekumar, *et al.* (1997), arXiv: 9709257 v1.

50. A. A. Abdo, *et al.* (1997), arXiv: 1003.3588 v2.

51. P. H. T. Tam, *et al.* (1997), arXiv: 1207.7267 v1.

52. M. T. Frandsen, *et al.* (2013), arXiv: 1304.6066 v2.

53. G. Agakishiev, *et al.* (2013), arXiv: 1311.0216 v1.

54. P. Fayet, Phys. Lett. **B 95**, 285 (1980).

55. C. Boehm, P. Fayet, Nucl. Phys. **B 683**, 219 (2004).

56. P. Fayet, Phys. Rev. **D 70**, 023514 (2004).

57. M. Pospelov, A. Ritz, M. B. Voloshin, Phys. Lett. **B 662**, 53 (2008).

58. N. Arkani-Hamed, D. P. Finkbeiner, T. R. Slatyer, , N. Weiner, Phys. Rev. **D 79**, 015014 (2009).

59. H. Merkel, *et al*., A1 Collaboration, Phys. Rev. Lett. **106**, 251802 (2011).

60. S. Abrahamyan, *et al*., APEX Collaboration, Phys. Rev. Lett. **107**, 191804 (2011).

61. R. Meijer, *et al*., SINDRUM I Collaboration, Phys. Rev. **D 45**, 1439 (1992).

62. P. Adlarson, *et al*., WASA-at-COSY Collaboration, Phys. Lett. **B 726**, 187 (2013).

63. F. Archilli, *et al*., KLOE-2 Collaboration, Phys. Lett. **B 706**, 251 (2012).

64. D. Babuski, *et al*., KLOE-2 Collaboration, Phys. Lett. **B 720**, 111 (2013).

65. D. Cahill, Radio galaxy discovery near Earth spurs more questions (May 23, 2014).

http://www.sciencewa.net.au/topics/space/item/2837-radio-galaxy-discovery-near-earth-spurs-more-questions

66. C. Boehm, P. Fayet, J. Silk (2003), arXiv: 0311143 v1.

67. C. Boehm, *et al.* (2003), arXiv: 0309686 v3.

68. S. D. Hunter, *et al.*, The Astrophysical Journal, **481**, 205, E240 (1997).

69. Yu. A. Golubkov, M. Yu. Khlopov (2000), arXiv: 0005419 v1.

70. B. Wolfe, *et al.* (2008), arXiv: 0807.0794 v1.

71. R. Yamazaki, *et al.* (2006), arXiv: 0601704 v2.

72. T. Nakamori (2008) www.heap.phys.waseda.ac.jp/cnf1203/Files/Oral/Nakamori.pdf

73. Y. Rasera, *et al.* (2006), arXiv: 0507707 v2.

74. A. A. Zdziarski, Mon. Not. R. Astron. Soc. **281**, L9 (1996).

75. D. E. Gruber, J. L. Matteson, and L. E. Peterson (1999), arXiv: 9903492 v1.

76. P. Gorenstein, R. Giacconi, and H. Gursky, The Astrophysical Journal, **150**, L85 (1967).

77. S. Safi-Harb, H. Ogelman, The Astrophysical Journal, **483**, 868 (1997).

78 T. Itoh, *Suzaku Studies of Time Variable X-ray Spectra of Edge-On Active Galactic Nuclei,* PhD Thesis(2007) http://www.astro.isas.jaxa.jp/suzaku/bibliography/phd/titoh_dron_print080220.pdf

79. A. M. Bykov, *et al.* (2009), arXiv: 0801.1255 v1.

80. R. Fukuoka, *et al.* (2008), arXiv: 0903.1906 v1.

81. A. Morretti, *et al.* (2012), arXiv: 1210.6377 v1.